PHYSICAL REVIEW B VOLUME 55, NUMBER 20 15 MAY 1997-II

# Role of silicon vacancies in yttrium-disilicide compounds from *ab initio* calculations

L. Magaud
*Laboratoire d'Etudes des Propriétés Electroniques des Solides, CNRS, 25 Avenue des Martyrs, Boîte Postale 166, F-38042 Grenoble, France*

A. Pasturel
*Laboratoire de Physique Numérique, CNRS, 25 Avenue des Martyrs, Boîte Postale 166, F-38042 Grenoble, France*

G. Kresse and J. Hafner
*Institut für Theoretische Physik, Technische Universität Wien, Wiedner Hauptstrasse 8-10, A-1040 Wien, Austria*

(Received 31 December 1996)

The structural properties of the compound $YSi_2$ are investigated by means of *ab initio* simulations based on density-functional theory. More particularly we emphasize the role played by Si vacancies, show that the $Th_3Pd_5$ structure can be deduced from the $AlB_2$ structure by a relaxation process around the Si vacancies within the (0001) plane. A specific ordered arrangement of the Si vacancies along the [0001] direction is found to be energetically the most favorable. Geometries obtained from our theoretical calculations are in good agreement with experimental results. [S0163-1829(97)06920-8]

## I. INTRODUCTION

Heavy rare-earth ($R$) (Gd-Lu) and Y disilicides ($R\mathrm{Si}_2$) are very special members of the silicide family. They have a very small lattice mismatch with Si(111) (0% for $YSi_2$) and can be epitaxially grown on this surface. The resulting interface is of high crystalline quality, similar to the ideal juxtaposition of two monocrystals. Their main technological interest comes from the very low Schottky barrier heights they exhibit on $n$-type Si: 0.3–0.4 eV compared to 0.6–0.8 eV for the other silicide-silicon interfaces.[1] They are then good candidates for fabrication of IR detectors in $n$-type silicon technology.

A hexagonal $AlB_2$-type structure was first described for a silicide of composition $Y_3Si_5$, but not for $YSi_2$.[2] A hexagonal silicide with $AlB_2$-type structure has the space group $P6/mmm$ with yttrium at (0,0,0) and silicon at $(\frac{1}{3},\frac{2}{3},\frac{1}{2})$ and $(\frac{2}{3},\frac{1}{3},\frac{1}{2})$ position (see Fig. 1). This produces a layered silicon structure between which the yttrium atoms form intermediate layers. However the Si-Si distance is smaller in the $YSi_2$ compound (2.22 Å) than in the diamond-bulk Si structure (2.35 Å). Along the (111) direction, diamond Si is made of a superposition of buckled Si layers. If a stress is applied to a buckled layer so that it becomes flat, the resulting Si plane is the one found in the $AlB_2$ structure. It is commonly admitted that the silicon planes in the rare-earth disilicides are constrained by the two adjacent $R$ planes. Therefore, the occurrence of Si vacancies may induce a relaxation of neighboring atoms which should increase the Si-Si distance and hence release part of the constraint.

Knapp and Picraux[3] demonstrated that numerous epitaxial $R$ disilicide films display a $R\mathrm{Si}_{1.7}$ stoichiometry in which one silicon atom out of every six is missing. A periodic rearrangement of these vacancies is possible, although this has not been definitely established. High-energy electron diffraction on epitaxial $ErSi_2$ films,[1,3,4] show a $\sqrt{3}\times\sqrt{3}$ $R30$ pattern which has been related to vacancy ordering in the (0001) planes. Very recently Lohmeier *et al.* measured the atomic displacements[5] from x-ray-diffraction analysis, and found that the structure is equivalent to the $Th_3Pd_5$ lattice with Si-Si bond lengths equal to the bulk Si interatomic distance. The corresponding unit cell is shown in Fig. 1. It is three times larger than that of $YSi_2$, and contains eight atoms: three Y and five Si. Two types of silicon sites appear: Si1 which has one vacancy in its first-neighbor shell, and Si2, which has the same first neighbors as in the $AlB_2$ structure. This structure is equivalent to the $Yb_3Si_5$ structure proposed by Iandelli, Palenzona, and Olcese.[6] The vacancies induce atomic relaxation and, because of the symmetry, only the Y and Si1 atoms move.

Another interesting feature is the organization of the vacancies along the $c$ axis. Baptist *et al.*[7] showed a 120° rotation between two successive Si planes in the $YSi_2$ compound. Thus only every second Si plane has the same orientation, and the period along [0001] is $2c$.

Up to now a complete theoretical treatment of these materials, showing the influence of the Si vacancies on the structural stability of $R\mathrm{Si}_2$ compounds, does not exist. Only band-structure calculations have been performed, using either the $AlB_2$ structure or the $Th_3Pd_5$ structure.[8–10] In the case of the $YSi_2$ compound, the main result is that the effect of vacancies is to shift the Fermi level toward a region of much lower density, which improves agreement between the $YSi_2$ theoretical density of states and x-ray-photoemission spectroscopy spectra. However, no energetic criterion has been used in these approaches, and the use of the atomic sphere approximation in Refs. 8 and 9 does not allow us to study the relaxation phenomenon related to the occurrence of vacancies, and its influence on the structural stability of $R\mathrm{Si}_2$ compounds.

Here we present the results of an extended *ab initio* density-functional-theory study of the structural properties of the $YSi_2$ compound which is performed using the Vienna *ab initio* simulation package (VASP).[11] We choose to study this

0163-1829/97/55(20)/13479(6)/$10.00

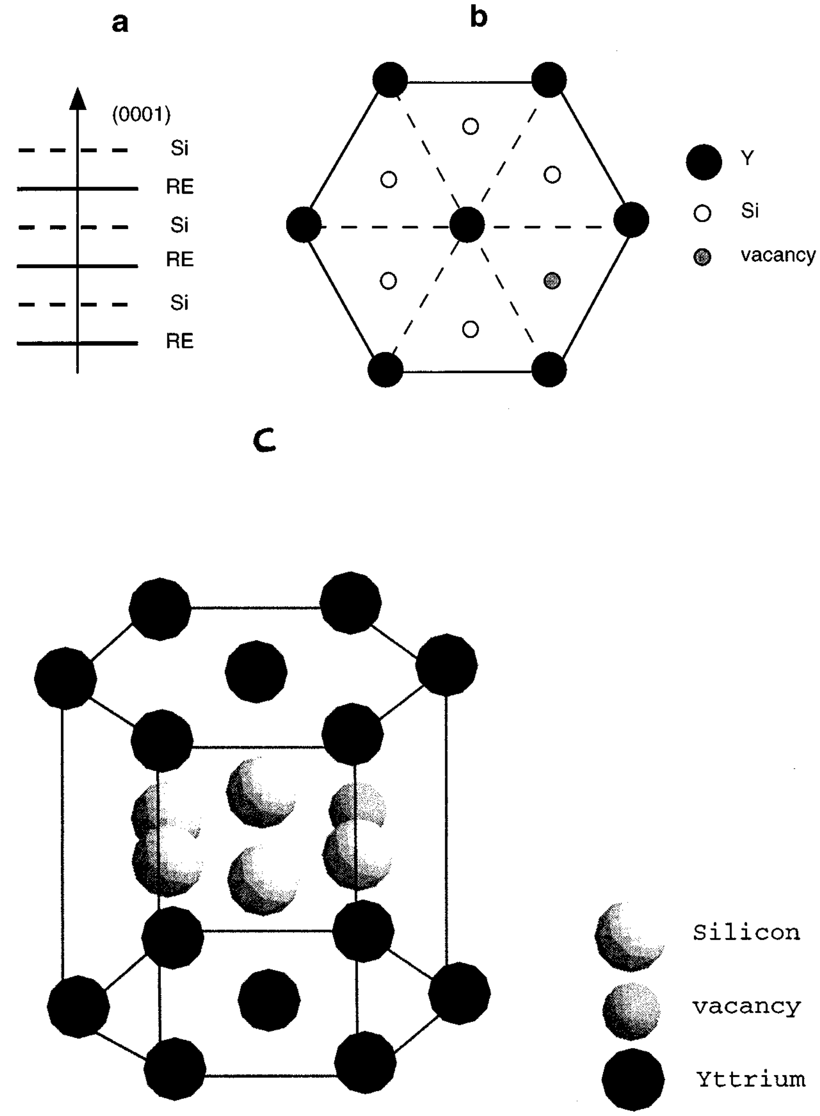

FIG. 1. $AlB_2$ structure (a) sequence of $R$ and Si planes along the $c(0001)$ axis, (b) projection on a (0001) plane, and (c) $AlB_2$ structure with a vacancy in the Si plane.

compound because the absence of $f$ electrons allow a pseudopotential approach. However even though Y has no $f$ electrons, the $YSi_2$ compound can be considered as a prototype compound for the $RSi_2$ series since it displays the same experimental properties as the other $R$ disilicides (Yb disilicide expected).

The paper is organized in the following way: Sec. II gives a description of the method, as well as some technical details of the calculations. The results concerning the structure and atomic positions optimization are presented in Sec. III. The vacancy ordering along the $c$ axis is also presented with discussions. Conclusions are summarized in Sec. IV.

## II. METHODS

For our investigation, we use VASP,[11] which is based on pseudopotentials. The construction method for these pseudopotentials[12] is derived from Vanderbilt's recipe for ultrasoft pseudopotentials.[13] These pseudopotentials allow the use of moderate-energy cutoffs even for systems containing $d$ transition elements (e.g., 200 eV for Y and $YSi_2$). For the actual calculation of ultrasoft pseudopotentials for Y and $YSi_2$, the chosen atomic reference configurations were $4p\,^6 5s\,^1 4d^2$ for Y and $3s\,^2 3p^2$ for Si. The ultrasoft pseudopotential of Si has already been used elsewhere,[14,15] and, for instance, it allows us to calculate phonon-dispersion relations with an accuracy of 3%.[15] For building ultrasoft pseudopotential for yttrium, we used two nonlocal projectors (i.e., two reference energies) per angular-momentum component; the cutoff radii are $R_{c,l}=3.43$, 3.10, and 3.43 a.u. for $l=2$, 1, and 0, respectively. The radii for the calculation of the augmentation functions are $R_{\mathrm{aug},l}=2.78$, 2.40, and 3.06 a.u. for $l=2$, 1, and 0, respectively. The truncated all-electron pseudopotential has been chosen as the local component. Partial core corrections[16] were introduced to enable a proper treatment of the nonlinear dependence of the exchange-correlation functional. With this choice of the pseudopotential, good plane-wave convergence can be achieved with a cutoff energy of $E_{\mathrm{cut}}=200$ eV. However, it is essential to include the $4p$ states as valence states in order to obtain correct lattice parameter for bulk structures.[17] A finite-temperature density-functional approximation is used to solve the generalized Kohn-Sham equations via an efficient iterative matrix diagonalization scheme based on a conjugate gradient technique. Within this framework, the free energy is the variational functional, and a fraction occupation

TABLE I. $c/a$ ratio for hcp structure, volume per atom $(V0)$, and the total-energy differences between fcc and hcp structures and bcc and hcp structures. APW is augmented plane wave.

| $c/a$ ratio | Theor. | Expt. (Ref. 23) | $V_0$ (A$^3$) | Theor. | Expt. (Ref. 23) | $\Delta E_{\text{fcc-hcp}}$ | (meV/atom) | $\Delta E_{\text{bcc-hcp}}$ | (mev/atom) |
|---|---|---|---|---|---|---|---|---|---|
| VASP | 1.564 | 1.572 | VASP | 30.1 | 33.03 | VASP | −0.008 | VASP | −0.135 |
| FPLMTO | 1.557 | 1.572 | FPLMTO | 30.1 | 33.03 | FPLMTO | −0.012 | FPLMTO | −0.139 |
| APW (Ref. 24) | 1.594 | 1.572 | APW (Ref. 24) | 30.1 | 33.03 | APW (Ref. 24) | −0.004 | | |

of the eigenstates is allowed which avoids the instability coming from the level crossing and quasidegeneracies in the vicinity of the Fermi level in metallic systems. Forces are calculated through the Hellmann-Feynman theorem as the variational derivatives of the free energy with respect to the atomic positions. The technique of Methfessel and Paxton[18] for the Fermi surface broadening is used. Since VASP allows for an analytical calculation of the forces and stresses, a geometry optimization can be readily carried out by again using the conjugate gradient method. After each geometry update, an extrapolation of wave functions is made to improve the input for the next step. For further technical details, we refer to Ref. 19.

### A. Bulk yttrium

In the present work, in order to check the accuracy of the pseudopotential, we applied it for the calculation of structural stability for bulk Y, and compared the results to data obtained by a full-potential linearized muffin-tin-orbital (FPLMTO) method.[20] The FPLMTO approach, which is an all-electron method and does not require any shape approximations for density and potential, is one of the most accurate *ab initio* state-of-the art methods. However, for a geometry optimization, it is less efficient than the pseudopotential approach, since forces are not available. As a first step we calculated the structural stability of bulk Y, namely, the total-energy differences between fcc and hcp structures and bcc and hcp structures; we also calculated the $c/a$ ratio and volume per atom $(V_0)$ for the hexagonal structure: Both sets of calculations were performed within the local-density approximation (LDA) of Ceperley and Alder.[21] Particular care was taken for the total-energy convergence due to the $k$-space integration, which in the present case was done by application of a special $k$-point technique.[18] The smearing parameter was chosen equal to 0.15. For the different structures the number of $k$ points in the irreducible part of the Brillouin zone were chosen in order to ensure that the total free energy is converged within 2 meV per atom. For the full-potential calculations, it is essential to use LMTO's with various localizations. In the present calculations we have used 41 augmented Hankel functions per Y site $[s(3\ \mathrm{K}),\ p(3\ \mathrm{K}),\ 3(d\ \mathrm{K})$, and $f(2\ \mathrm{K})]$, where the corresponding decay energies are $-K^2=-0.01$ $(spdf)$, $-1.0$ $(spdf)$, and $-2.3$ Ry $(spd)$. The charge density is calculated exactly in the muffin-tin spheres in angular momentum components up to $l=6$. We use the same angular momentum cutoff in the interpolation of quantities in the interstitial region, expanded in Hankel functions of energies $-1$ and $-3$ Ry.[22] Accurate calculations of the bulk properties require also an extended treatment of the Y 4$p$ states. We have therefore included a second ''semicore'' panel to provide bandlike representation of both the Y 4$s$ and 4$p$ states, using the same Y basis as for the upper panel, except for the appropriate reduction in the Y $s$ and $p$ principal quantum numbers.

From Table I, we find a good agreement between the two calculated sets of values. Because of the shortcomings of the LDA, the calculated volume per atom is smaller than the experimental result.[23] Let us mention that our data are also in good agreement with the ones provided by Sigalas and Papaconstantopoulos.[24]

### B. $YSi_2$ in the $AlB_2$ structure

Within the same spirit, we performed both FPLMTO and VASP calculations for the $YSi_2$ compound in the $AlB_2$ structure. The structural parameters $c/a$ and $a$ have been optimized, leading to $c/a=0.967$ and 0.975, respectively, for VASP and FPLMTO methods, and $a=4.044$ and 4.066, respectively, for VASP and FPLMTO. In both cases we obtained lattice parameters which are rather different from the experimental values $(a=3.842,\ \ c/a=1.077)$, and especially a ratio $c/a$ smaller than one for the theoretical approaches. We have checked that the behavior of the $c/a$ ratio does not depend on the volume at which the calculations have been performed. It may be thought that the introduction of vacancies in the silicon plane may introduce structural variations in the $AlB_2$ structure and more particularly a variation of the $c/a$ parameter. It is the purpose of Sec. III to explore such variations.

## III. INFLUENCE OF VACANCIES ON STRUCTURAL PROPERTIES OF $YSi_2$ COMPOUND

In this section we will use only results based on VASP, as we are interested in the influence of vacancies on the structural stability of the $YSi_2$ compound; in this case it is essential to take into account the relaxation process induced by these defects, as will be shown below.

### A. $AlB_2$ structure

The first step is to introduce one Si vacancy out of six atoms of Si in the $AlB_2$ structure. This results in a $\sqrt{3}\times\sqrt{3}$ $R30$ supercell. We performed a geometry optimization, namely, the optimization of the corresponding shape and the volume of the cell, but with no atomic displacement. In this case, the obtained lattice parameters, i.e., $a=3.964$,

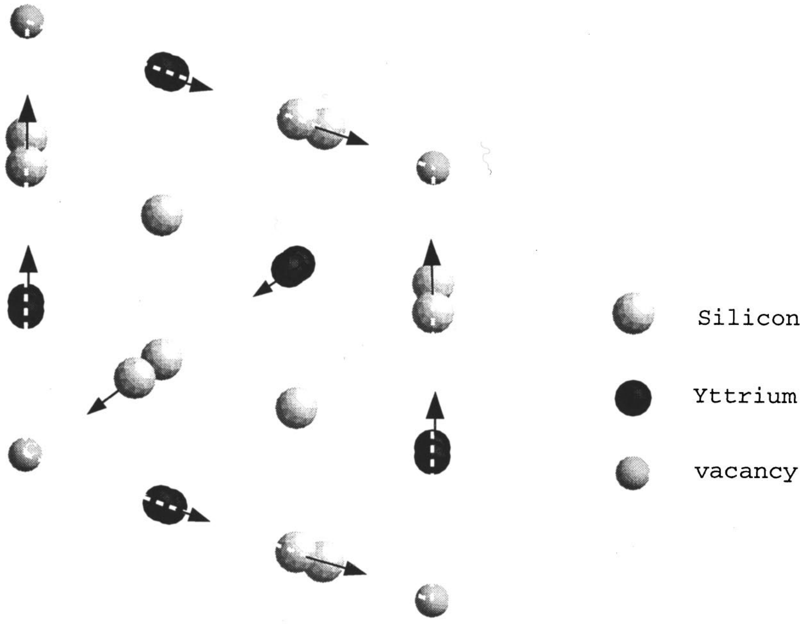

FIG. 2. Relaxation of yttrium and silicon atoms in the (0001) plane; arrows indicate the moves of the atoms from the $AlB_2$ structure to the $Th_3Pd_5$ structure.

and $c/a = 0.984$, are close to the experimental values, but the $c/a$ remains smaller than 1. In fact, the introduction of a silicon vacancy divides silicon atoms in two types, vacancy first neighbors (type-1 Si1) and others (type-2 Si2). The presence of a vacancy may induce a relaxation of the neighboring atoms. From symmetry reasons, it is easy to see that Si2 will not move. We then let the atoms move, and we optimize the shape and the volume of this cell. Type-1 Si atoms move toward the vacancy, while Y atoms move away from it (see Fig. 2). Let us mention that although all the degrees of freedom are authorized during the ionic relaxation, the Si1 and Y atoms move only in the [0001] planes. This relaxation leads to a structure similar to the $Th_3Pd_5$ structure, as proposed by Iandelli, Palenzona, and Olcese.[6] In this structure, the atomic positions depend on two parameters $x$ and $x'$. The thorium (or yttrium) atom is located at $(x,0,0)$, and palladium atoms (or Si1 and Si2 atoms) are at $(x',0,\frac{1}{2})$ and $(\frac{1}{3},\frac{2}{3},\frac{1}{2})$, respectively. From Table II, it can be seen that the lattice parameters obtained after relaxation are in better agreement with the experimental values. The $x$ and $x'$ values obtained from the numerical relaxation are in close agreement with the values proposed in Ref. 6 for the $Yb_3Si_5$ compound. The displacement of Si atoms around the vacancy leads to a decrease of the value of the $a$ lattice parameter and an increase of the $c/a$ ratio. But the main consequence of these displacements is to increase the Si-Si distance and hence to release a part of the constraint imposed by the two adjacent Y planes.

TABLE II. Lattice parameters, volume, and atomic displacements with respect to the $AlB_2$ structure. All parameters are expressed with respect to an undistorted $AlB_2$ structure.

| System | $a$ (Å) | $c/a$ | $V$ (Å$^3$) | $x$ (Å) | $x'$ (Å) |
|---|---|---|---|---|---|
| $YSi_2$ (expt.) | 3.842 | 1.0786 | 52.974 | | |
| $YSi_2$ ($AlB_2$) | 4.044 | 0.967 | 55.38 | | |
| $YSi_{1.7}$ ($AlB_2$) | 3.964 | 0.984 | 53.08 | 0.333 | 0.666 |
| $YSi_{1.7}$ ($Th_3Pd_5$) | 3.759 | 1.082 | 49.73 | 0.354 | 0.733 |
| $Yb_3Si_5$ Ref. 6 | 3.784 | 1.083 | 50.817 | 0.358 | 0.745 |

The occurrence of the Si vacancies in the $AlB_2$ structure leads to the $Th_3Pd_5$ structure after relaxation, and also has consequences on the ground-state properties of the Y-Si system. In Figure 3 we plot the calculated values of the formation energies of the compounds in the Si-rich side of the phase diagram, namely, the $YSi_2$ compound in the $AlB_2$ and $Th_3Pd_5$ structures, and the YSi-compound in the orthorhombic CrB-type structure. The formation energies of all the compounds are defined as

$$\Delta E^{\text{form}} = E^{T}_{\mathrm{Y}_x\mathrm{Si}_{1-x}} - xE^{T}_{\mathrm{Y}_{\mathrm{hcp}}} - (1-x)E^{T}_{\mathrm{Si}_{\mathrm{dia}}}.$$

All these structures are characterized by strong negative values of the formation energies, showing that the Y-Si system displays strong chemical interactions between Y and Si at-

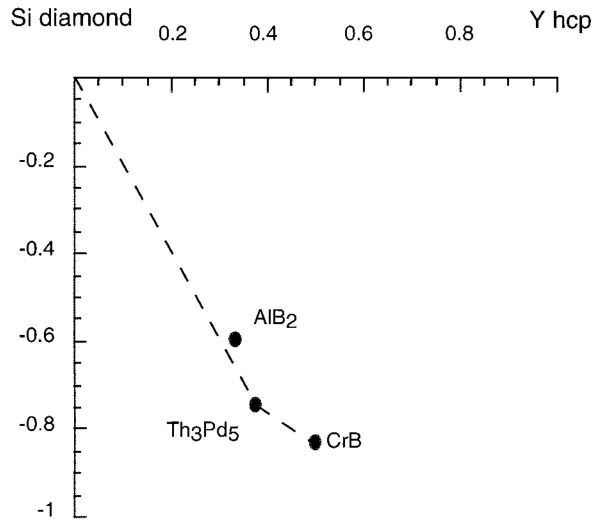

FIG. 3. Ground-state analysis in the Si-rich part of the Y-Si phase diagram.

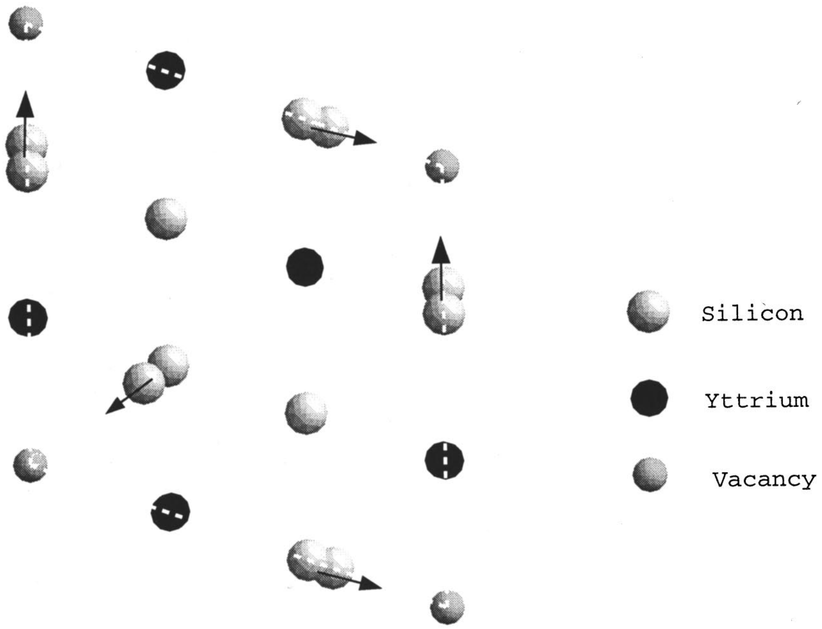

FIG. 4. Relaxation of the yttrium and silicon atoms in (0001) plane; arrows indicate the moves of atoms from the $AlB_2$ structure to the $2c$- 120°-rotated structure.

oms. A previous analysis of the $AlB_2$ structure[9,25] showed that these interactions are mainly due to the coupling of the Y $d$ orbital and the Si $p$ orbital. It is very interesting that the conclusion is that the $AlB_2$ structure is unstable with respect to the equilibrium Si (diamond) $\rightleftarrows$ $Th_3Pd_5$; indeed, the formation energy of the $AlB_2$ structure is just below the line drawn between Si (diamond) and $Th_3Pd_5$ structures, as seen from Fig. 3; this means that the $AlB_2$ structure does not occur at $T=0$ K. It is in complete agreement with thermal analysis, metallography, and x-ray diffraction,[26] which show that the $YSi_2$ compound does not form at all as a stable phase at this composition.

### B. Long-range ordering of vacancies along *c* axis

In Sec. III A, we showed that the introduction of silicon vacancies in the hexagonal $AlB_2$ structure leads to a relaxation of the surrounding Si atoms and the occurrence of a $Th_3Pd_5$-type crystallographic structure. These calculations assumed periodic conditions along the $c$ axis with a periodicity equal to $c$. This means that the vacancies are superimposed along the $c$ axis. This might not be the case since the vacancies can be rotated from one Si plane to the other one. Indeed, Baptist *et al.*[7] showed by low-energy electron diffraction (LEED) that the next Si plane is rotated by 120° around [0001]. More recently, Frangis *et al.* emphasized the occurrence of the modulated structures in erbium disilicide-thin films grown on a Si(111) substrate using electron microscopy characterization (HREM).[27] Among these modulated structures, high-resolution images confirm the presence of the $2c$-layer sequence but also a $3c$-layer sequence.

In order to investigate these different possibilities, we first doubled the length of the cell along the $c$ axis so that the unit cell now includes two Si and Y planes, and only every second plane has the same orientation. Three different configurations are possible, namely 0°, 60°, and 120° rotation of the Si vacancy from one Si plane to the other one. The first case (0° rotation) is equivalent to previous calculations, but we did it for the double-$c$ cell to perform all the calculations using the same numerical strategy (number of $k$ points, namely, 48 $k$ points in the irreducible part of the Brillouin zone). The 120° rotation of the Si vacancies appears to be the most stable configuration at $T=0$ K. Its energy is 30 meV per vacancy more negative than the superposition configuration, and 10 meV per vacancy more negative than the 60° rotation one. The atomic relaxation according to the rotation angle leads to different behaviors for Y and Si atoms. For symmetry reasons, atomic positions are identical in the two Y planes, and each silicon plane has two fixed silicon atoms. In the case of the superposition configuration, the Y atoms display significant displacements (0.13 Å) while, for the 60° and 120° rotations, Y positions are close to the unrelaxed values. For the Si1 atoms, the displacements ar rather similar for 0° and 120° configurations 0.43 and 0.38 Å, respectively (see Fig. 4). Let us mention that these displacements just happen in the (0001) plane; single and double-$c$ cell calculations never show any displacement of the Si1 (or Y) atoms along the $c$ axis.

We then performed $3c$ supercell calculations including 0° and 120° configurations. In this latter configuration, the Si vacancies are rotated by 120° between each Si plane, resulting in a $3c$ periodicity. This $3c$ 120° rotated configuration is found to be more stable than the $2c$ 120° rotated configuration. The change in energy is 20 meV per vacancy. This difference is quite small, and it can be easily understood that, during thermal treatments of these materials, several modulated structures can occur. The main important point is that the presence of these modulated structures can be attributed to the nonstoichiometry of the material.

## IV. CONCLUSION

The influence of silicon vacancies on the structure of the yttrium disilicide compound has been studied using an efficient *ab initio*-based geometry-optimization approach. The use of ultrasoft pseudopotentials allows us to treat the quite localized $d$ electrons of Y and then to have an analytical calculation of the Hellmann-Feynman forces and stresses.

This greatly facilitates the geometry optimization using conjugate gradient techniques.

We showed that without vacancies, the calculated lattice parameters of the equilibrium $AlB_2$-type cell geometry are different from the experimental ones, especially with a ratio $c/a$ smaller than 1. The introduction of a vacancy in the Si plane induces a relaxation of its first- (Si) and second- (Y) neighbor atoms and a variation of the cell geometry, e.g., the equilibrium $a$ and $c/a$ values are then much closer to the experimental ones. This new configuration can be interpreted within a $Th_3Pd_5$-type structure. The main characteristic of this structure is that a part of the constraint on the Si atom in the $AlB_2$ structure is released by relaxation process. The consequence is that the $AlB_2$ structure is unstable with respect to the equilibrium Si (diamond)$\rightleftarrows$ $YSi_2$ ($Th_3Pd_5$). Double- and triple-$c$-cell calculations found that vacancies are in fact rotated by 120° in two or three successive silicon planes along the [0001] direction, as observed by LEED measurements[7] or in HREM images.[27] However, a rotated configuration cannot be strictly described by the $Th_3Pd_5$-type structure. The small energy differences found in our calculations lead to the presence of modulated structures in these materials. As the lattice parameters are very sensitive to the presence and ordering of vacancies in the silicon sublattice, it may be thought that the vacancies are at the origin of the very good epitaxial properties of the $RESi_2$ compounds on a Si(111) substrate.

## ACKNOWLEDGMENT

This work was supported by a computer grant at the Institut de Développement et des Ressources en Informatique Scientifique (IDRIS-CNRS).

---

[1] J. Y. Duboz, P. A. Badoz, A. Perio, J. C. Oberlin, F. Arnaud d'Avitaya, Y. Campidelli, and J. A. Chroboczek, Appl. Surf. Sci. **38**, 171 (1989).

[2] C. E. Lundin, in *The Rare Earths*, edited by F. H. Spedding and A. H. Daane (Wiley, New York, 1961), p. 265.

[3] J. A. Knapp and S. T. Picraux, Appl. Phys. Lett. **48**, 466 (1986).

[4] F. Arnaud d'Avitaya, A. Perio, J. C. Oberline, Y. Campidelli, and J. A. Chroboczek, Appl. Phys. Lett. **54**, 2198 (1989).

[5] M. Lohmeier, W. J. Huisman, E. Vlieg, A. Nishiyama, C. L. Nicklin, and T. S. Turner, Surf. Sci. **345**, 247 (1996).

[6] A. Iandelli, A. Palenzona, and G. L. Olcese, J. Less-Common Met. **64**, 213 (1979).

[7] R. Baptist, S. Ferrer, G. Grenet, and H. C. Poon, Phys. Rev. Lett. **64**, 311 (1990).

[8] G. Allan, I. Lefebvre, and N. G. Christensen, Phys. Rev. B **48**, 8572 (1993).

[9] L. Magaud, J. P. Julien, and F. Cyrot-Lackmann, J. Phys. Condens. Matter **4**, 5399 (1992).

[10] L. Stauffer, C. Pirri, P. Wetzel, A. Mharchi, P. Paki, D. Bolmont, G. Gewinner, and C. Minot, Phys. Rev. B **46**, 13 201 (1992).

[11] G. Kresse and J. Hafner, Phys. Rev. B **47**, 558 (1993); G. Kresse, Ph.D. thesis, Technische Universität Wien, 1993.

[12] G. Kresse and J. Hafner, J. Phys. Condens. Matter **6**, 8245 (1994).

[13] D. Vanderbilt, Phys. Rev. B **41**, 7892 (1990).

[14] R. Stadler, W. Wolf, R. Podloucky, G. Kresse, J. Furthmüller, and J. Hafner, Phys. Rev. B **54**, 1729 (1996).

[15] C. Demuth, G. Kresse, G. Kern, and J. Hafner (unpublished).

[16] S. G. Louie, S. Froyen, and M. L. Cohen, Phys. Rev. B **26**, 1738 (1982).

[17] B. J. Min and K. M. Ho, Phys. Rev. B **40**, 7532 (1989).

[18] M. Methfessel and A. T. Paxton, Phys. Rev. B **40**, 3616 (1989).

[19] G. Kresse and J. Furthmüller, Comput. Mater. Sci. **6**, 15 (1996); Phys. Rev. B **54**, 11 169 (1996).

[20] M. Methfessel, Phys. Rev. B **38**, 1537 (1988).

[21] D. Ceperley and D. Alder, Phys. Rev. Lett. **45**, 566 (1980); J. P. Perdew and A. Zunger, Phys. Rev. B **23**, 5048 (1981).

[22] A. T. Paxton, M. Methfessel, and H. M. Polatoglou, Phys. Rev. B **41**, 8127 (1990).

[23] *Pearson's Handbook of Crystallographic Data*, 2nd ed., edited by P. Villars and L. D. Calvert (American Society for Metals, Metals Park, OH, 1991).

[24] M. M. Sigalas and D. A. Papaconstantopoulos, Phys. Rev. B **50**, 7255 (1994).

[25] L. Magaud, J. Y. Veuillen, D. Lollman, T. A. Nguyen Tan, D. A. Papaconstantopoulos, and M. Mehl, Phys. Rev. B **46**, 1299 (1992).

[26] T. W. Button, I. J. McColm, and J. M. Ward, J. Less-Common Met. **159**, 205 (1990).

[27] N. Frangis, G. Van Tendeloo, J. Van Landuyt, P. Muret, and T. T. A. Nguyen, Appl. Surf. Sci. **102**, 163 (1996).